British Journal of Cancer

ARTICLE

Check for updates

Cellular and Molecular

AMPK phosphorylates and stabilises copper transporter 1 to synergise metformin and copper chelator for breast cancer therapy

Xiaomei Zhang[1,2,3], Qiwei Jiang[2,3], Yaqing Su[2], Lang Bu[2], Zicheng Sun[1,2], Xueji Wu[2], Bing Gao[2], Lei Wang[2], Ying Lin[1✉], Wei Xie[2✉] and Jianping Guo[2✉]

BACKGROUND: Predominant roles of copper and its transporter, copper transporter 1 (CTR1), in tumorigenesis have been explored recently; however, the upstream regulation of CTR1 and combinational intervention of copper chelators in malignancies remain largely unclear.

METHODS: CRISPR/Cas9-based kinome screening was used to identify the CTR1 upstream kinases. Immunofluorescence assays were utilised to detect CTR1 localisation. In vitro kinase assays and mass spectrometry were performed to detect CTR1 phosphorylation. Ubiquitination assays were performed to validate CTR1 stability. Colony formation, EdU labelling, Annexin V-FITC/PI-based apoptosis assays were carried out to detect the drug effect on cell growth and apoptosis. Xenografted mouse models were employed to investigate drug effects in vivo.

RESULTS: We identify that CTR1 undergoes AMPK-mediated phosphorylation, which enhances CTR1 stabilisation and membrane translocation by affecting Nedd4l interaction, resulting in increased oncogenic roles in breast cancer. Importantly, activation of AMPK with its agonist metformin markedly enhances CTR1 levels, and leads to the combinational usage of AMPK agonists and copper chelators for breast cancer treatment.

CONCLUSIONS: Our findings not only reveal the crosstalk between energy response and copper uptake via AMPK-mediated CTR1 phosphorylation and stability but also highlight the strategy to combat breast cancer by a combination of AMPK agonists and copper chelators.

SIGNIFICANCE: The connection between energy response and copper homoeostasis is linked by AMPK phosphorylating and stabilising CTR1, which provides a promising strategy to combat breast cancer by combining AMPK agonists and copper chelators.

British Journal of Cancer (2023) 128:1452–1465; https://doi.org/10.1038/s41416-022-02127-4

INTRODUCTION

Breast cancer is now the most frequent malignancy worldwide. Based on the presence of molecular markers for estrogen receptor (ER)/progesterone receptor (PR) and human epidermal growth factor 2 (HER2), breast cancers have been categorised into three major subtypes including ER-positive, HER2-positive, and triple-negative breast cancer (TNBC) [1]. Noteworthily, although only approximately 15% of all breast tumours belong to TNBC, they exhibit a relatively high risk of metastasis and recurrence, as well as poor prognosis, coupled with lacking targeted therapy [2–4]. Thus, huge efforts have been devoted for exploring the strategies for TNBC intervention. For example, TNBC patients bearing *BRCA* mutations display deficient DNA damage repair [5], leading to clinical response to the poly (ADP-ribose) polymerase (PARP) inhibitors [6]. In addition, phosphatidylinositol-3-kinase (PI3K) inhibitors have been successfully employed for *PIK3CA*-mutated cancers, and immunotherapeutic targeted PD-L1 blockage has also been applied in TNBC [6, 7]. However, despite initial responses to these therapies, TNBC commonly becomes prone to metastasis and relapse due to its heterogeneity [4]. Hence, it is necessary and urgent to establish and develop novel targeted interventions for TNBC.

Apart from genetic factors, unbalanced trace elements are closely associated with breast cancer risk [8]. Copper, an essential trace element, serves as a key component in a number of copper-dependent enzymes; therefore, dysregulation of copper has been remarkedly involved in multiple pathologic processes [9]. Interestingly, higher copper levels have been observed in either serum or tumour tissues of breast cancer patients [8, 9], and copper also plays a critical role in tumour cells and their

[1]Department of Breast and Thyroid Surgery, the First Affiliated Hospital, Sun Yat-sen University, Guangzhou, Guangdong 510275, China. [2]Institute of Precision Medicine, the First Affiliated Hospital, Sun Yat-sen University, Guangzhou, Guangdong 510275, China. [3]These authors contributed equally: Xiaomei Zhang, Qiwei Jiang.
✉email: Linying3@mail.sysu.edu.cn; Xiew56@mail.sysu.edu.cn; guojp6@mail.sysu.edu.cn

Received: 2 August 2022 Revised: 9 December 2022 Accepted: 15 December 2022
Published online: 17 February 2023

microenvironments [10], which supports copper depletion as an attractive therapeutic strategy [10]. For example, copper could bind mitogen-activated protein kinase kinase 1 (MEK1) [11], 3-phosphoinositide-dependent protein kinase 1 (PDK1) [12], unc-51-like kinase 1/2 (ULK1/2) [13] to contribute to tumorigenesis of melanoma, breast and non-small cell lung cancer (NSCLC) respectively. Recently, intra-tumoral copper reveals an important role in regulating PD-L1 expression to influence tumour immune evasion [14]. Hence, depleting *CTR1* or chelating copper to deprive intratumor copper has provided a vital treatment strategy for tumour immunotherapy. As such, copper chelators ammonium tetrathiomolybdate (TTM) and disulfiram (DSF) have begun to apply as anti-cancer agents in cancer clinical trials [15]. For instance, orally bioavailable TTM is now undergoing a Phase II clinical study, and shows a potential benefit for survival in advanced TNBC patients [15].

As a key cellular energy sensor, AMP-activated protein kinase (AMPK), is an important hub of metabolic homoeostasis, a hallmark of cancer. AMPK activation has been considered as a promising strategy for treating metabolic diseases including diabetes, obesity and cancers [16]. Remarkably, AMPK exhibits functions on reducing breast cancer cell proliferation [17], and enhancing apoptosis in breast cancer mouse models [18], which provides the rational for employing AMPK activators, such as metformin for breast cancer therapy [19]. As a result, diabetic patients who have received metformin administration, display a relatively lower risk of breast cancer incidence possibly due to the activation of AMPK [20]. Unexpectedly, although metformin exhibits unique anti-TNBC actions both in vitro and in vivo [21], long-term metformin utilisation fails to show any relevance with breast cancer prognosis [22], possibly due to acquired drug resistance. For example, cross-resistance to metformin and tamoxifen was induced via constitutive activation of AKT/Snail/E-cadherin signalling in breast cancer cells [23]. Thus, revealing the underlying mechanisms of resistance to metformin and developing purposeful strategies to overcome this resistance are in urgent need. In this report, via a CRISPR/Cas9-based approach for screening CTR1 upstream regulatory kinase(s), we identify that AMPK directly phosphorylates and stabilises CTR1 to promote copper uptake and activating downstream oncogenic signals, providing a promising strategy by a combination of metformin and TTM for breast cancer therapy.

RESULTS

CRISPR/Cas9-based screening for CTR1 upstream regulatory kinase

Due to the critical roles of CTR1 in copper uptake and subsequently promoting tumorigenesis [11–13], we tended to determine whether CTR1 is undergoing a kinase-dependent turnover regulation. To this aim, we set up a CRISPR-based screen system as we previously reported [24]. Briefly, constructs encoding GFP-fusion CTR1 and separated expression of RFP were stably expressed and further infected with CRISPR/Cas9-based kinome viruses. After selecting and sorting with GFP and RFP, the kinases enhancing CTR1 protein levels were identified, among which PRKAA1 (AMPKα1) was ranged as one of the top kinases (Fig. 1a, b). In keeping with this finding, increased CTR1 abundance in protein but not mRNA levels were validated in wild-type (WT) but not kinase-dead (KD, K45R) AMPKα1-overexpressing cells, accompanied with decreased well-established copper readout protein, copper chaperone for superoxide dismutase (CCS) levels [25–27] (Fig. 1c, d and Supplementary Fig. S1a, b).

Next, we observed that pathologically activated AMPK by employing AMPK agonists such as metformin, A-769662 and AICAR dramatically promoted CTR1 protein abundance and reduced CCS levels in both HEK293T and breast cancer MDA-MB-231 cells (Fig. 1e, f and Supplementary Fig. S1c). Consistently, activated AMPK could not increase CTR1 mRNA levels (Supplementary Fig. S1a), and alter the formation of CTR1 homodimer (Supplementary Fig. S1d), a functional status for copper uptake. In accordance with this finding, CTR1 expression was prominently reduced in *Ampka1/2* double knockout MEFs and breast cancer BT-549 cells (Fig. 1g), independent of CTR1 mRNA levels (Supplementary Fig. S1e). To further reveal whether AMPK could elevate CTR1 in protein level, CTR1 half-lives were detected, and showed that depletion of *Ampka* apparently shortened CTR1 half-life (Fig. 1h), while activation of AMPK markedly prolonged CTR1 half-life (Supplementary Fig. S1f), indicating that AMPK modulates CTR1 at least in part by enhancing its protein stability. Furthermore, restored the catalytic components of AMPK including AMPKα1 and AMPKα2, both enhanced endogenous CTR1 expression, coupled with decreased CCS levels (Fig. 1i). More importantly, to evaluate the correlation of AMPK activation and CTR1 expression, we detected the phosphorylation of acetyl-CoA carboxylase 1 (ACC1), a canonical marker for AMPK activation [28], and elevated CTR1 expression was observed significantly correlated with the activation of AMPK in breast tumour tissues (Fig. 1j, k). These findings together suggest that AMPK enhances CTR1 protein stability.

AMPK enhances CTR1 membrane translocation

As a major copper transporter, CTR1 mainly resides and functions in plasma membrane [29–34]. To this end, we sought to investigate whether AMPK could enhance CTR1 membrane localisation. Of note, AMPK activators such as metformin and AICAR indeed enhanced CTR1 membrane localisation observed by cell fractionation and immunofluorescence assays (Fig. 2a–d and Supplementary Fig. S2a–d). Moreover, AMPK activation induced by deprivation of glucose or treated with 2-DG physiologically (Fig. 2a, b), by treated with metformin or AICAR pathologically (Fig. 2a–d and Supplementary Fig. S2a–d), and by enforced expression of AMPKα (Fig. 2e–h and Supplementary Fig. S2e), all markedly enhanced CTR1 membrane localisation, which was obviously antagonised by AMPK inhibitor Compound C (Comp C) (Fig. 2c, d and Supplementary Fig. S2a–f) or expressing the kinase-dead AMPKα1 (K45R) (Fig. 2e–g). Consistent with these findings, restoring the catalytic component AMPKα1 could markedly enhance endogenous CTR1 membrane localisation (Fig. 2h). These findings together suggest that activation of AMPK contributes to CTR1 membrane localisation.

AMPK directly interacts with and phosphorylates CTR1

As a serine/threonine kinase, AMPK has been revealed to phosphorylate many substrates and plays distinct roles in metabolic homoeostasis and tumorigenesis [35, 36]. With the predominant effect of AMPK on CTR1 protein levels, we sought to detect whether AMPK could interact with and phosphorylate CTR1. To this end, the interaction of AMPKα1 and CTR1 was initially performed, and AMPKα1 was identified to bind CTR1 in cells (Fig. 3a). Interestingly, a potential AMPK phosphorylation motif was nailed down in CTR1 cytoplasm region (Fig. 3b). Via an in vitro kinase assay coupled with mass spectrometry (MS) analysis, S105 residue within the cytoplasm region of CTR1 was identified as a potential AMPK phosphorylation site (Fig. 3c), while substitution of S105 to A105 markedly attenuated AMPK-induced CTR1 phosphorylation detected with the AMPK substrate phosphorylation antibody (Supplementary Fig. S3a). To further elucidate this phosphorylation event under physiological conditions, we generated and validated specific antibodies against phosphorylated S105-CTR1 (Supplementary Fig. S3b). As a result, activation or ectopic expression of AMPK markedly elevated CTR1 phosphorylation in S105 (Fig. 3d, e), whereas inhibiting AMPK pharmacologically or enforced expression kinase-dead AMPK obviously abrogated CTR1-S105 phosphorylation (Fig. 3d, e and Supplementary Fig. S3c, d). These findings suggest that CTR1 is a bona fide substrate of AMPK.

In common, the phosphorylation of serine is well mimicked by substituting to aspartic acid (D) or glutamic acid (E), whereas non-phosphorylation of serine is mimicked with alanine (A) [37].

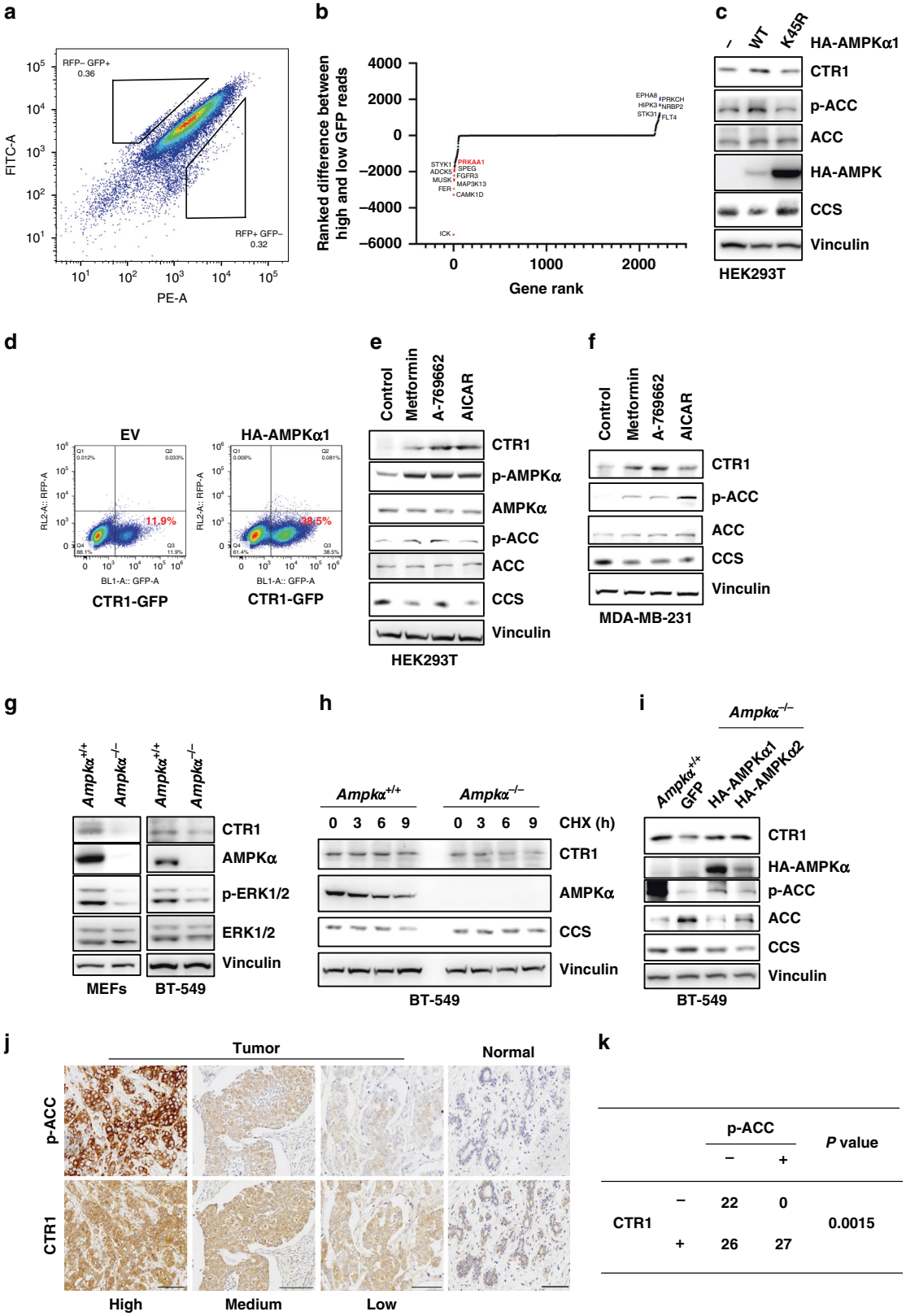

However, if the modified residue resides in the critical structure region, its substitution would like to artificially change the protein conformation and functions, leading to loss of function after (non)-phosphomimic substitution. This phenomenon was observed in CTR1 phosphorylation site in S105. In this setting, although S105 was validated to be phosphorylated by AMPK, S105A substitution markedly blocked AMPK and its agonists induced CTR1 phosphorylation (Fig. 3f–j). Simultaneously, CTR1 expression and membrane localisation induced by ectopic expression of AMPKα1 or activation of AMPK could be counteracted by S105A mutant, coupled with

Fig. 1 AMPK enhances CTR1 protein levels. a, **b** Screening the kinase(s) stabilising CTR1 via a CRISPR/Cas9 system using high-throughput sequencing. **c** Immunoblot (IB) analysis of whole cell lysate (WCL) derived from HEK293T cells transfected with the indicated constructs. **d** Flow cytometry analysis of CTR1 expression for HEK293T cells transfected with the indicated constructs. **e**, **f** HEK293T and MDA-MB-231 cells were treated with AMPK agonists including metformin (20 mM), A-769662 (200 μM), and AICAR (1 mM), respectively, for 3 h and then subjected to IB analyses. **g** IB analyses of WCL derived from *Ampkα*$^{-/-}$ and counterpart MEFs and BT-549 cells. **h** IB analysis of WCL derived from *Ampkα*$^{-/-}$ and counterpart BT-549 cells treated with indicated time course of CHX (100 μg/ml). **i** BT-549-*Ampkα*$^{-/-}$ cells were infected with lentiviruses encoding indicated proteins and then selected with hygromycin (100 μg/ml) for 5 days, the resulting and WT cells were subjected to IB analysis. **j**, **k** Image representation of immunohistochemistry (IHC) for CTR1 expression and ACC1 phosphorylation in different breast cancer tissues from TMA (**j**). The correlation of CTR1 expression and ACC1 phosphorylation was calculated and analysed using χ^2 analysis ($P < 0.05$) (**k**). Bar indicates 100 μm.

reverse changes of CCS levels (Fig. 4a–e). Unexpectedly, S105A-CTR1 still displayed a relatively high membrane localisation capability compared with intact CTR1 (Fig. 4c–e). Moreover, in the functional studies, both S105A and S105D CTR1 exhibited prolonged half-lives compared with WT CTR1 (Supplementary Fig. S3e), and enhanced CTR1 membrane translocation (Supplementary Fig. S3f), with no effect on CTR1 dimer formation (Supplementary Fig. S3g). These observations indicate that AMPK-mediated phosphorylation of S105 is important for CTR1 stability and membrane localisation; however, S105A or S105D substitution could not well mimic the non-phosphorylation or phosphorylation status of CTR1 respectively, which limited the utilisation of these mutations to evaluate the phosphorylation effect on CTR1-mediated AMPK functions.

AMPK phosphorylates CTR1 to abrogate Nedd4l-mediated ubiquitination

Due to the previous finding that CTR1 undergoes Nedd4l-mediated ubiquitination and degradation [12], and AMPK stabilises CTR1, we sought to detect whether AMPK could affect Nedd4l-mediated CTR1 degradation. To this end, ectopic expression of AMPKα1 apparently repressed the interaction between CTR1 and Nedd4l (Fig. 5a). Consistent with this finding, metformin and AICAR repressed, whereas Compound C enhanced CTR1/Nedd4l interaction (Fig. 5b, c). To test whether AMPK-mediated phosphorylation affects CTR1/Nedd4l interaction, we observed that AMPK expression, metformin or AICAR treatment-reduced CTR1/Nedd4l interaction was largely elevated upon administration of lambda-phosphatase (λ-phosphatase) (Fig. 5d–f). Consistently, AMPK and its agonists repressed Nedd4l-mediated CTR1 ubiquitination, resulting in elevated CTR1 stability (Fig. 5g–i). Meanwhile, ubiquitin-conjugation of endogenous CTR1 in *AMPKα*-depleted BT-549 cells was largely increased, which was attenuated by re-introducing AMPKα (Supplementary Fig. S3h). These observations indicate that AMPK stabilises CTR1 by blocking its interaction with the E3 ubiquitin ligase Nedd4l, and inhibiting Nedd4l-mediated CTR1 ubiquitination.

Copper chelator synergises with AMPK agonists for breast cancer therapies

AMPK is commonly considered as a tumour suppressor in different cancer settings; thus, its agonist metformin has been broadly applied in clinical studies for cancer therapies [38, 39]. However, metformin displays an unsatisfactory benefit for certain cancer therapies, including breast cancer. Here we showed that AMPK and its activators could enhance the phosphorylation and stability of CTR1, which facilitates copper uptake and exerts a critical role in drug resistance or cell growth in breast cancer by activating MAPK or AKT pathways [11, 12], which will contribute to the resistance of metformin. Thus, we raised the question that whether targeting copper-CTR1 axis could synergise with metformin for cancer therapy. To this end, we first employed copper chelator TTM, which has been exploited in clinical trials for melanoma [40], thyroid cancer [41], and breast cancer [15], and observed that *AMPK* knockout significantly decreased TTM functions in repressing cell proliferation and enhancing cell apoptosis (Supplementary Fig. S4a–c). In addition, TTM enhanced WT but not *CTR1*-deficient breast cancer cell apoptosis (Supplementary Fig. S4d–g), while re-introduction of CTR1 restored *CTR1*-deficient breast cancer cell response to TTM (Supplementary Fig. S4h, i), indicating that TTM functions in anti-tumour growth indeed by chelating CTR1-mediated copper transportation. Interestingly, *CTR1* depletion diminished synergistic effect of metformin with TTM for promoting breast cancer apoptosis (Supplementary Fig. S4d–g), suggesting that AMPK-mediated elevation of CTR1-copper axis is an acquired target for breast cancer therapy. To validate the combination of AMPK agonist and copper chelator, we treated breast cancer cells with metformin, and observed that metformin activated AMPK signalling coupled with increased cellular copper levels as indicated by the decrease of CCS (Supplementary Fig. S4j), leading to cellular response to copper chelator TTM treatment (Supplementary Fig. S4f–i).

To investigate the sensitivity of metformin or TTM for different breast cancer cells, the IC_{50} for different breast cancer cells was measured (Supplementary Fig. S5). Subsequently, concentrations of metformin or TTM lower than IC_{50} were selected for exploring their synergic effect (Supplementary Tables S1 and S2). As a result, breast cancer cells exhibited more sensitivity to the combinational administration of metformin and TTM in repressing cell viability (Fig. 6a, b and Supplementary Fig. S6a), cell proliferation (Fig. 6c, d and Supplementary Fig. S6b), colony formation (Fig. 6e, f and Supplementary Fig. S7a–d), and elevated cell apoptosis (Fig. 6g, h and Supplementary Fig. S8e). To exclude the broad functions of metformin in AMPK-independent manner, we also employed another AMPK agonist, AICAR for functional studies. The results showed that, similar to metformin, AICAR also could synergise with TTM to markedly repress breast cancer cell viability, proliferation and promote cell apoptosis (Supplementary Fig. S8a–d). Finally, to explore the synergic roles of these two drugs in vivo, tumours derived from breast cancer cells were further challenged with administration of metformin and TTM individually or in combination. The result showed that these two drugs played robustly synergic roles in suppressing breast cancer tumour growth, coupled with decreased cell proliferation index Ki-67 with tolerable side effects (Fig. 7a–j and Supplementary Fig. S9a–d). In addition, TTM has also been reported to repress breast cancer migration [42]; thus, the combination of TTM and metformin indeed detectably suppressed breast cancer invasion and migration (Supplementary Fig. S10a, b). These findings together suggest that metformin-mediated AMPK activation will promote CTR1 expression, which sensitises the cells to copper chelators.

DISCUSSION

As a hallmark of cancer, tumour metabolic homoeostasis is attracting more attention these years, among which, energy-related regulations by AMPK in tumorigenesis are predominantly focused [36]. AMPK, considered as a tumour suppressor, could be activated by metformin, a drug widely used for diabetes [43], now broadly applied for cancer therapies [44]. Unexpectedly, some studies indicate that AMPK also exerts oncogenic roles under certain conditions to help tumour cells tolerate energy deprivation [35, 45–49]. Here, via a CRISPR/Cas9-based screening, we identify

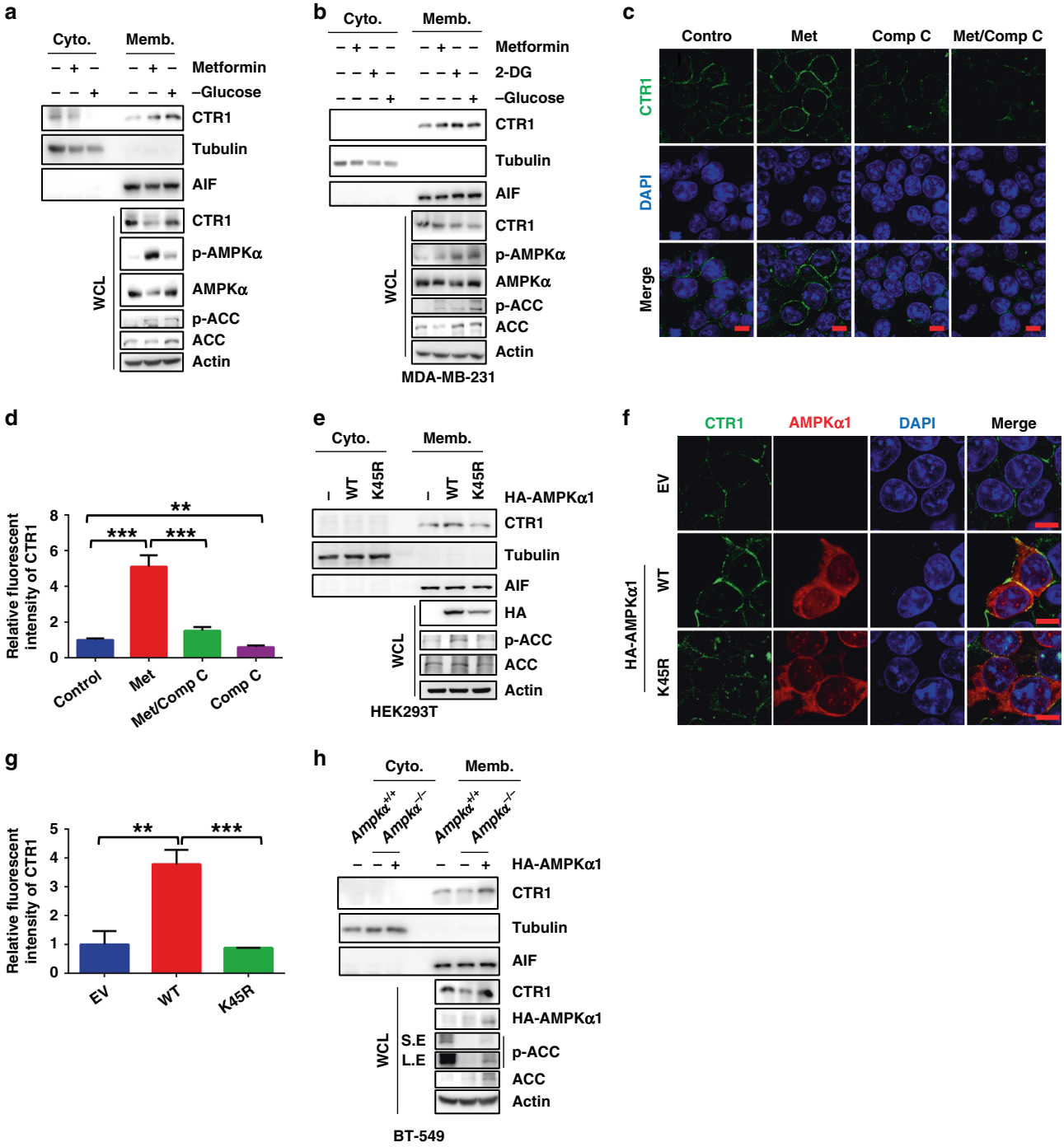

Fig. 2 AMPK activation facilitates CTR1 membrane location. a, **b** HEK293T (**a**) and MDA-MB-231 (**b**) cells were treated with AMPK agonists metformin (20 mM), 2-DG (10 mM) or glucose-starved for 6 h, respectively and then subjected to cell fractionation and IB analyses. **c**, **d** HEK293T cells were treated with AMPK agonist metformin (20 mM) and AMPK inhibitor Compound C (2.5 μM) for 6 h, resulting cells were fixed and then subjected to immunofluorescence (IF) analysis (**c**), the relative fluorescent intensity of CTR1 was analysed (**d**) (mean ± SD, $n = 3$). $^{*}P < 0.05$, $^{**}P < 0.01$ (Student's *t*-test). Bar indicates 10 μm. **e** HEK293T cells were transfected with AMPK WT and kinase-dead mutant, and then subjected to cell fractionation and IB analyses. **f**, **g** HEK293T cells were transfected with the indicated constructs and then subjected to immunofluorescence (IF) analysis (**f**), the relative fluorescent intensity of CTR1 was analysed (**g**) (mean ± SD, $n = 3$). $^{*}P < 0.05$, $^{**}P < 0.01$ (Student's *t*-test). Bar indicates 10 μm. **h** BT-549-*Ampka*$^{-/-}$ cells were infected with lentiviruses encoding indicated proteins and then selected with hygromycin (100 μg/ml) for 5 days, the resulting cells were subjected to cell fractionation and IB analysis. S.E. and L.E. indicate short exposure and long exposure, respectively.

that AMPK physiopathologically elevates CTR1-copper axis, leading to its downstream oncogenic signalling activation, which possibly contributes to cellular tolerance to energy deprivation. However, whether elevated CTR1-copper axis-induced metabolic alterations contribute to this process is desired to be further explored. On the other hand, although metformin has been clinically or preclinically employed for cancer therapies, less response and acquired resistance commonly occur for distinct

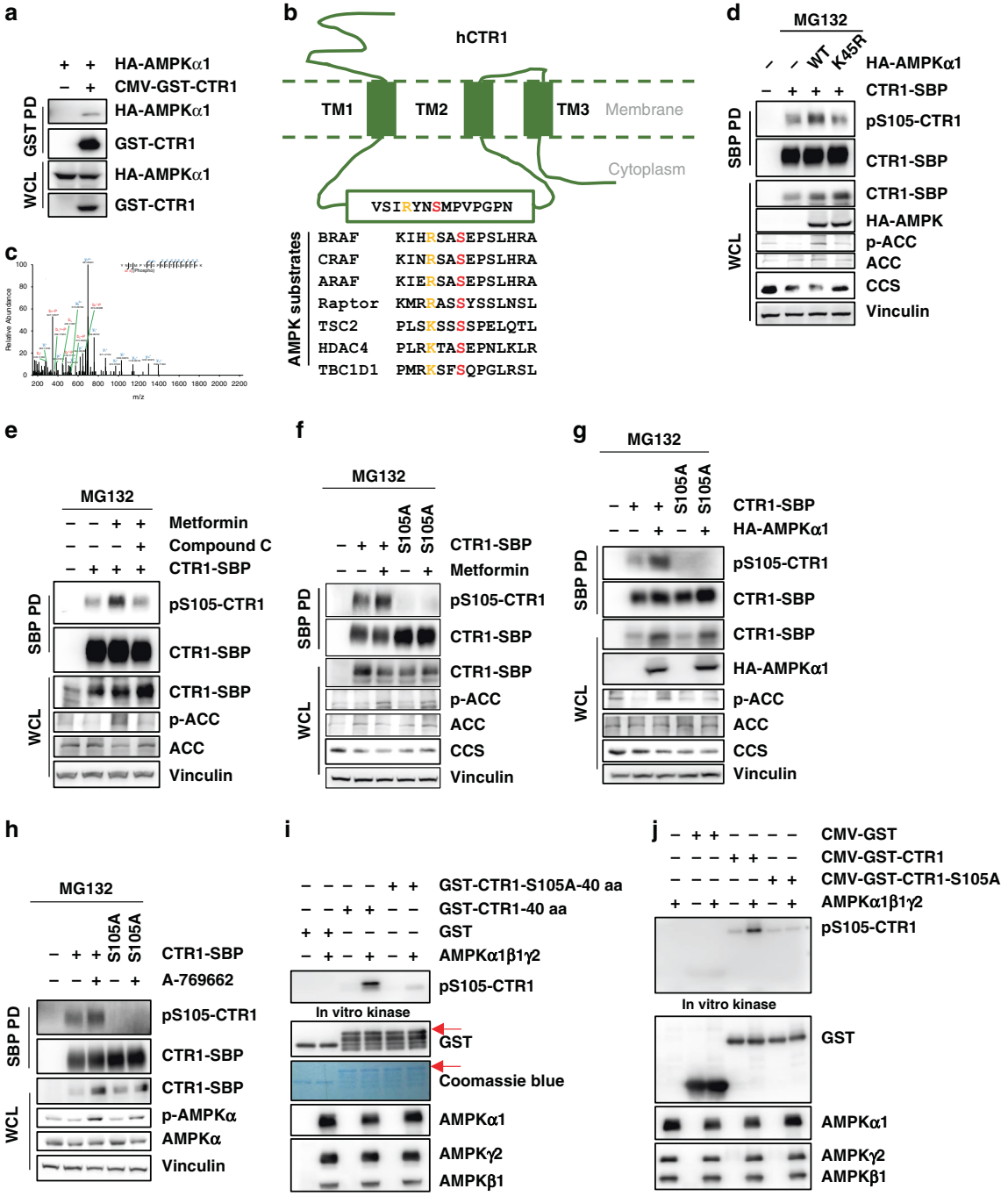

Fig. 3 AMPK directly phosphorylates CTR1. a HEK293T cells were transfected with indicated constructs, then the resulting cells were subject to immunoprecipitation (IP) analysis. **b** Primary structure of CTR1 (top panel). Amino acid sequence analysis of CTR1 and certain AMPK substrates (bottom panel). **c** HEK293T cells were transfected with indicated constructs and then treated with MG132 (10 μM) for 12 h, resulting cells were harvested for mass spectrometry analysis. **d**, **e** HEK293T cells were transfected with indicated constructs and then treated with metformin (20 mM), Compound C (2.5 μM), and MG132 (25 μM) for 6 h, the resulting cells were harvested and subject to IP and IB analyses. **f**–**h** HEK293T cells were transfected with indicated constructs and then treated with metformin (20 mM), A-769662 (200 μM), and MG132 (25 μM) for 6 h, respectively, resulting cells were harvested and subject to IP and IB analyses. **i**, **j** In vitro kinase assays were performed with recombinant AMPKα1β1γ2 as the source of kinase and bacterially purified (**i**) or cellular purified (**j**) CTR1 as the substrates, the products were subject to IB analysis.

reasons. Due to the fact that pathological activation of AMPK by its agonists such as metformin and A-769662 in cancer or diabetes therapies, will promote copper transportation and activating downstream MAPK and AKT pathways [11, 12], possibly resulting in resistance to metformin-mediated cancer therapies (Fig. 7k).

Copper chelator TTM has been exploited for cancer therapies, mainly focusing on the *BRAF*^{V600E} mutant melanoma [40], thyroid [41] and breast [15] cancers, due to the capability of copper directly activating the driver genes, such as MEK and Memo/AKT, respectively. However, given the potential side effects, single use of TTM has displayed unsatisfactorily for cancer intervention. Of note, previous studies also reveal that TTM could function as a chemosensitizer by increasing apoptosis of malignant cells in combination with cytotoxic chemotherapeutic agent doxorubicin

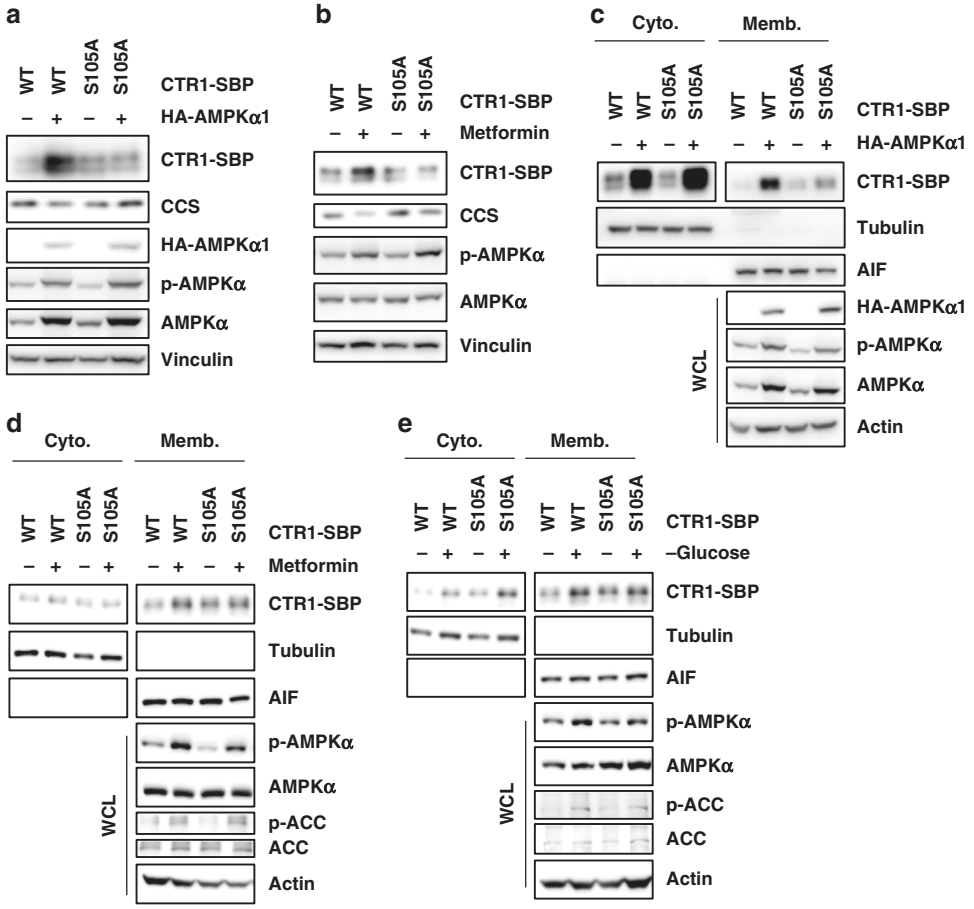

Fig. 4 AMPK-mediated CTR1 phosphorylation affects its protein level and localisation. a, **b** HEK293T cells were transfected with indicated constructs and then treated with metformin (20 mM) for 6 h, resulting cells were subjected to IB analyses. **c**–**e** HER293T cells were transfected with indicated constructs and then treated with metformin (20 mM) and glucose-starved for 6 h, respectively, and then subject to cell fractionation and IB analyses.

[50]. Due to the CRISPR screening result, we have identified that the tumour suppressor AMPK exhibits a 'side effect' to elevate CTR1-copper axis, an oncogenic pathway in diverse cancers. To this end, administration of AMPK agonist will unexpectedly elevate CTR1-copper signalling, which provides the strategy for the combination of AMPK agonist metformin with copper chelator TTM for breast cancer therapies, which has been initially validated both in cells (Fig. 6 and Supplementary Figs. S6 and S7) and in xenograft mouse models (Fig. 7a–j). However, previous study also reported that copper chelator TTM could also activate AMPK [42]; thus, whether there is a potential feedback regulation around AMPK-CTR1-copper axis is warrant to further investigation.

Due to the limitation of detecting copper concentration and CTR1 expression, the usage of copper chelator for cancer therapies has been markedly restricted. Here, we show the broadly used AMPK agonist metformin could strongly induce CTR1 expression, and they display a tight association in breast cancer patients, which provides us a marker by detecting AMPK activity for utilising copper chelator for breast cancer therapies. More recently, non-copper transporter roles of CTR1 have also been identified to mediate VEGFR2 function in promoting angiogenesis via ROS-induced CTR1 cysteine oxidation [51]. Here we show that CTR1 undergoes AMPK-mediated phosphorylation upon energy deprivation or metformin administration. Thus, elevated CTR1 will engage its oncogenic functions via both copper-dependent and -independent roles. As such, only deprivation of copper with its chelators will be not enough to diminish CTR1 oncogenic functions, therefore, specific antibodies or PROTAC approaches will be developed to leash oncogenic roles of CTR1. In summary, our findings not only reveal the fine-tuned regulation of CTR1 stabilisation by AMPK-mediated phosphorylation, but also highlight the promising strategy via combinational usage of AMPK agonists and copper chelators for tumour therapies, especially for TNBC therapies.

METHOD AND MATERIALS

Cell lines, transfection and infection

HEK293T cells were cultured in HyClone Dulbecco's Modified Eagle Medium (DMEM) supplemented with 10% foetal bovine serum (FBS), penicillin (100 units) and streptomycin (100 μg/ml). BT-549 *Ampka*$^{-/-}$ and counterpart BT-549 *Ampka*^{WT}, MEFs *Ampka*$^{-/-}$ and MEFs *Ampka*^{WT} were obtained from Dr Wei (Beth Israel Deaconess Cancer Cetner). These cells were maintained in DMEM medium supplemented with 10% FBS. MDA-MB-231-LUC-D3H2LN cells were kindly provided by Dr Junchao Cai (Sun Yat-sen University), cultured in DMEM medium with 10% FBS. Breast cancer cell lines including MCF-7, T47-D, BT-474, ZR-75-30, SKBR-3, BT-549, MDA-MB-453, MDA-MB-231, MDA-MB-468 were cultured in RPMI 1640 medium or DMEM medium supplemented with 10% FBS and kept in our lab. Cell transfection was performed using Lipofectamine or PEI (Polysciences) according to the manufacturer's instructions. Packaging of knock-down or over-expression viruses, as well as subsequent infection of various cell lines were performed according to the methods described previously [12]. After viral infection, cells were maintained with different concentrations of

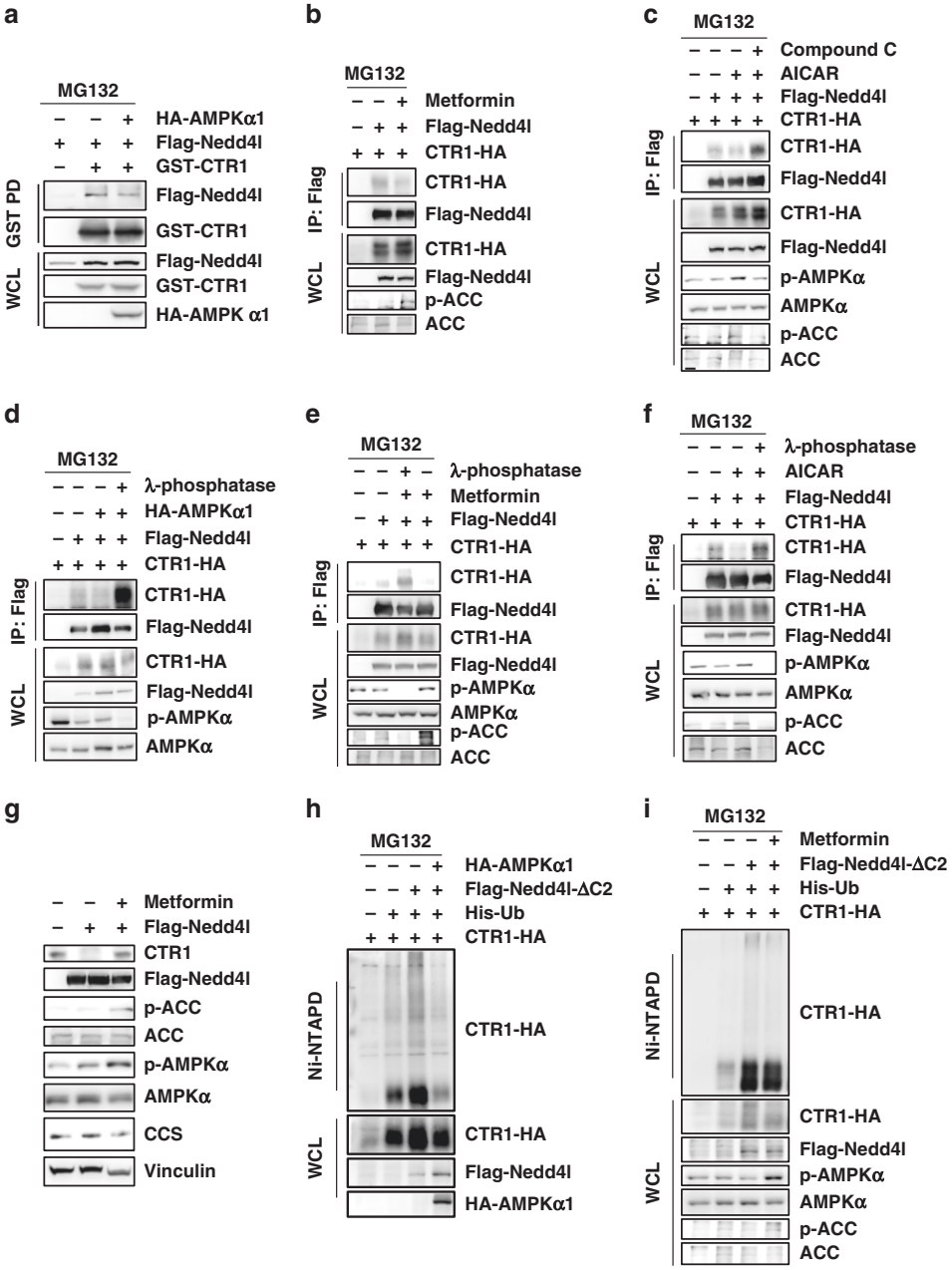

Fig. 5 AMPK activation blocks Nedd4l-mediated CTR1 degradation. a, **b** HEK293T cells were transfected with indicated constructs and then treated with metformin (20 mM) and MG132 (25 μM) for 6 h, the resulting cells were subject to IP and IB analyses. **c** HEK293T cells were transfected with indicated constructs and then treated with AICAR (1 mM), Compound C (2.5 μM) and MG132 (25 μM) for 6 h, the resulting cells were subject to IP and IB analyses. **d**–**f** HEK293T cells were transfected with indicated constructs and then treated with metformin (20 mM), AICAR (1 mM), and MG132 (25 μM) for 6 h, respectively, and the resulting cells were harvested and incubated with λ-phosphatase and then subject to IP and IB analyses. **g** HEK293T cells were transfected with indicated constructs and then treated with metformin (20 mM) for 6 h, and the resulting cells were harvested and subject to IB analysis. **h**, **i** HEK293T cells were transfected with indicated constructs and then treated with metformin (20 mM), AICAR (1 mM), and MG132 (25 μM) for 6 h, respectively, and the resulting cells were harvested and subject to Ni-NTA beads pull-down (PD) and IB analyses.

hygromycin or puromycin, depending on cell lines and the viral vectors used to infect cells.

Antibodies and reagents

All antibodies were used at a 1:2000 dilution in TBST buffer with 5% bovine serum albumin (BSA) for western blot. Anti-CTR1 antibody (13086), anti-phospho-Ser79-ACC antibody (11818), anti-ACC1 antibody (3676), anti-phospho-Thr172-AMPKα antibody (50081), anti-AMPKα antibody (5831), anti-phospho-ERK1/2 antibody (4370), anti-ERK1/2 antibody (4695), anti-β-Tubulin (2128) antibody, anti-AIF (5318) antibody, anti-phospho-Akt Substrate (RXXS*/T*) antibody (9614), anti-Caspase-3 antibody (14220), anti-PARP-antibody (9532), anti-Cleaved PARP antibody (5625), anti-Ubiquitin antibody (3933), anti-rabbit IgG (H+L), F(ab')$_2$ Fragment (Alexa Fluor® 488 Conjugate) (4412), and anti-mouse IgG (H+L), F(ab')$_2$ Fragment (Alexa Fluor® 594 Conjugate) (8890) were obtained from Cell Signaling Technology. Anti-Thiophosphate ester antibody (ab92570) was obtained from Abcam. Anti-CTR1 polyclonal antibody (NB100-402) was obtained from Novus Biologicals. Anti-CCS antibody (22802-1-AP) and anti-GST-tag antibody (66001-1-Ig) were obtained from

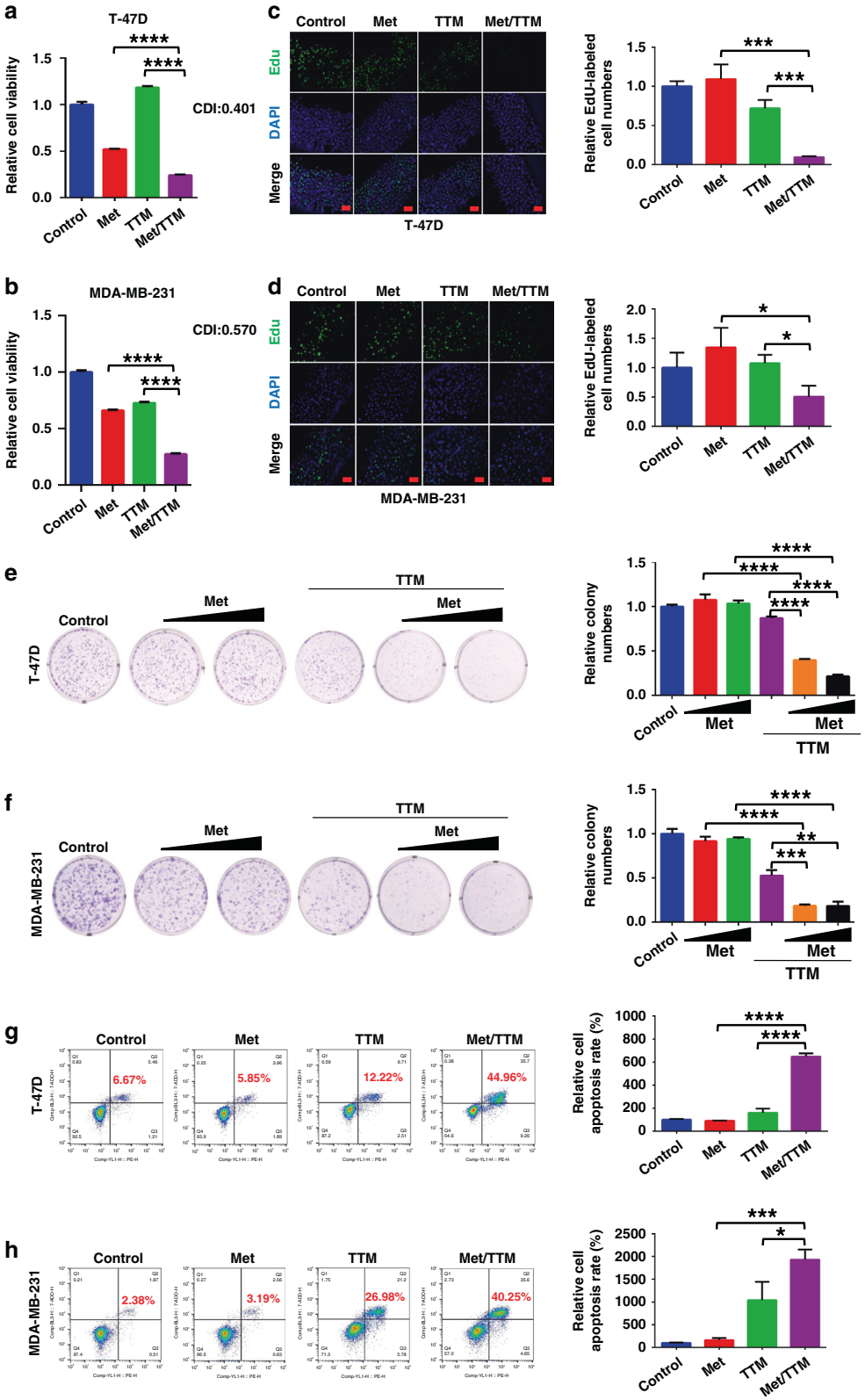

Proteintech. Anti-Vinculin antibody (V4505), monoclonal anti-Flag antibody (F-3165, clone M2), anti-Flag-M2 affinity gel (A2220) were obtained from Sigma. Anti-Actin antibody (sc-69879) and protein A/G plus-agarose (sc-2003) were obtained from Santa Cruz. Monoclonal anti-HA antibody (901503) was obtained from BioLegend. Streptavidin agarose (20353) was obtained from Thermo Fisher Scientific. Glutathione-Sepharose 4B (17-0756-05) was obtained from GE Healthcare. Ni-NTA agarose (30230) was obtained from QIAGEN. Peroxidase-conjugated anti-mouse secondary antibody (115-035-003) and peroxidase-conjugated anti-rabbit secondary antibody (111-035-003) were obtained from Jackson ImmunoResearch. Peroxidase-conjugated mouse anti-rabbit IgG LCS (A25022,

Fig. 6 Metformin synergises with copper chelator TTM in breast cancer cells. a, **b** T-47D and MDA-MB-231 cells were treated with indicated concentrations of metformin and TTM individually or in combination for indicated time point, then the cell viabilities were detected and analysed (mean ± SD, $n = 3$). *$P < 0.05$, **$P < 0.01$ (Student's *t*-test). Coefficient of drug in interaction (CDI) was calculated. CDI < 1 means synergistic effect, CDI < 0.7 means a significantly synergistic effect. **c**, **d** T-47D and MDA-MB-231 cells were treated with indicated concentrations of metformin and TTM individually or in combination for 24 h, and the resulting cells were fixed and labelled with EdU, relative EdU-labelled cell numbers were normalised and plotted (**c** and **d**, right panel) (mean ± SD, $n = 3$). *$P < 0.05$, **$P < 0.01$ (Student's *t*-test). Bar indicates 100 μm. **e**, **f** T-47D and MDA-MB-231 cells were treated with different concentrations of metformin and TTM individually or in combination for indicated time point, the resulting cells were fixed and stained with crystal violet solution, relative colony numbers were normalised and plotted (**e** and **f**, right panel) (mean ± SD, $n = 3$). *$P < 0.05$, **$P < 0.01$ (Student's *t*-test). **g**, **h** T-47D and MDA-MB-231 cells were treated with indicated concentrations of metformin and TTM individually or in combination for 48 h, the resulting cells were subjected to Annexin V-FITC/PI-labelled apoptosis assays, apoptotic cells were quantified (**g** and **h**, right panel) (mean ± SD, $n = 3$). *$P < 0.05$, **$P < 0.01$ (Student's *t*-test).

1:10,000) was obtained from Abbkine. The polyclonal antibodies against phospho-S105-CTR1 were generated by ABclonal Technology from rabbits. The antigen sequence utilised for immunisation was CTR1 aa102-109 (RYNS*MPVP). S* represents phosphorylated residue in this synthetic peptide.

AMPK agonists including metformin (S1950), A-769662 (S2697), AICAR (S1802), 2-DG (S4701), and AMPK inhibitor Compound C (S7840), MG132 (S2619) were obtained from Selleck. Gibco DMEM without glucose (11966025) was purchased from Thermo Fisher Scientific. DOX (D1515) and TTM (323446) were purchased from Sigma. $CuSO_4$ (C805782) was purchased from Macklin.

DNA constructs and mutants

To carry out kinome screening, the fragment CTR1-GFP-IRES-RFP obtained by overlap extension PCR was cloned into mammalian expression vector pLenti-Hygro. The fragments CTR1-GFP, CTR1-S105A-GFP, and CTR1-S105D-GFP acquired by overlap extension PCR were cloned into the vector pcDNA3.1. HA-AMPKα1, HA-AMPKα2, HA-AMPKα1-K45R, CTR1-HA, CTR1-S105A-HA, and CTR1-S105D-HA were inserted into the vectors pcDNA3.1 and pLenti-Hygro, respectively. CTR1, CTR1-S105A, and CTR1-S105D were inserted into the vectors pcDNA3-Strep-Flag and pCMV-GST, respectively. AMPKβ1 and AMPKγ2 were cloned into the vector pCMV-GST. Constructs of pcDNA3-Flag-Nedd4l, pcDNA3-Flag-Nedd4l-ΔC2, His-ubiquitin, and pLKO-shCTR1-tet-on were previously described [12]. pGEX-4T-CTR1 and pGEX-4T1-CTR1-S105A were cloned into indicated vectors. Details of plasmid constructions are available upon request. All plasmids were generated using the QuikChange XL Site-Directed Mutagenesis Kit (Stratagene) according to the manufacturer's instructions.

CRISPR-based kinome screening

The lentiviral vector pLenti-hygro-CTR1-GFP-IRES-RFP was packaged into viruses to infect and integrate into HEK293T cells. Under hygromycin selecting, the stable clones were obtained after 7 days. Following infection with CRISPR-Cas9 kinase lentivirus library [52], the clones were selected by treated with puromycin for 7 days to establish stable clones. The stable clone cells were sorted and collected by flow cytometry according to the fluorescent intensity of GFP. The collected high and low GFP cells were used for genomic DNA extraction and further carried out for high-throughput sequencing. Compared with the amplified sgRNAs in CRISPR library, the corresponding genes were ranked.

Immunoblotting (IB) and immunoprecipitation (IP) analysis

Cells were lysed in EBC lysis buffer (50 mM Tris pH 7.5, 120 mM NaCl, 1% NP-40) supplemented with protease inhibitors (Complete Mini, Roche) and phosphatase inhibitors (phosphatase inhibitor cocktail set I and II, Calbiochem). The cell lysates were resolved by SDS-PAGE and immunoblotted with indicated antibodies. For immunoprecipitation analysis, the lysates were incubated with distinct agarose beads conjugated with SBP, Flag or GST at 4 °C for 2–8 h. The immuno-complexes bound to beads were washed four times with NETN buffer (20 mM Tris, pH 8.0, 150 mM NaCl, 1 mM EDTA and 0.5% NP-40) and then were resolved by SDS-PAGE and immunoblotted with indicated antibodies. To immuno-precipitate the endogenous proteins, the cell lysates were incubated with the indicated antibody and Protein A/G Sepharose beads at 4 °C overnight. The beads were washed six times with NETN buffer following being resolved by SDS-PAGE. Quantification of the immunoblot band intensity was performed with ImageJ software.

Breast tumour microarrays (TMA) and immunohistochemical (IHC) staining

Tissue array (BC081120d) containing 10 cases of adjacent normal breast tissues, 100 cases of invasive ductal carcinoma were obtained from Biomax. The detailed procedures of immunohistochemistry were performed as previously reported [12]. Sections were incubated with anti-phospho-Ser79-ACC antibody (1:100) and anti-CTR1 polyclonal antibody (1:250). T-47D xenograft or MDA-MB-231 xenograft was sliced with 4 micron-thick, formalin-fixed paraffin-embedded sections. Sections were incubated with anti-phospho-Thr172-AMPKα antibody (1:100) and anti-Ki-67 antibody (1:100). All staining intensities were assessed and recorded by a quantitative imaging method.

Peptide synthesis and dot blotting assay

CTR1-WT and CTR1-S105-phospho peptides synthesised by ABclonal were used for dot blot assays. The sequences of peptides were the following: CTR1-WT: RYNSMPVP-C, CTR1-pS105: RYN(pS)MPVP-C. The peptides were diluted with PBS into the amount of 0.1, 0.2 and 0.3 μg and spotted onto nitrocellulose membrane before being incubated with polyclonal anti-phospho-S105-CTR1 antibody for immunoblot analysis.

Immunofluorescence (IF) and cell fractionations

Cells inoculated on glass coverslips were transfected with indicated plasmids and were disposed by distinct reagents at the indicated time points. Then the cells were fixed with 4% paraformaldehyde at room temperature (RT) for 15 min, washed twice with PBS and then permeabilised with 0.05% Triton X-100 at RT for 10 min. After washing three times with PBS, the cells were blocked with 5% BSA for 30 min and then incubated with anti-HA antibody (1:200) or anti-CTR1 antibody (1:200) at 4 °C overnight. Next, the cells were washed three times and incubated with anti-rabbit IgG (H+L), F(ab')2 Fragment (Alexa Fluor® 488 Conjugate) (1:500) or anti-mouse IgG (H+L), $F(ab')_2$ Fragment (Alexa Fluor® 594 Conjugate) (1:500) for 1 h at RT. After washing three times, the cells were stained with DAPI and analysed using confocal microscope ZEISS LSM880. Quantification of the fluorescent intensity was performed with ImageJ software. Cell fractionations were performed with Cell Fractionation Kit (CST, 9038) following the instructions.

mRNA extraction and qPCR

Total RNA was extracted using a phenol-chloroform method with TRIzol regent (Takara, 9109), and then reverse-transcribed using the Superscript RT kit (Takara, 6210A) according to the manufacturer's instructions. Quantitative Real-time PCR was performed using the

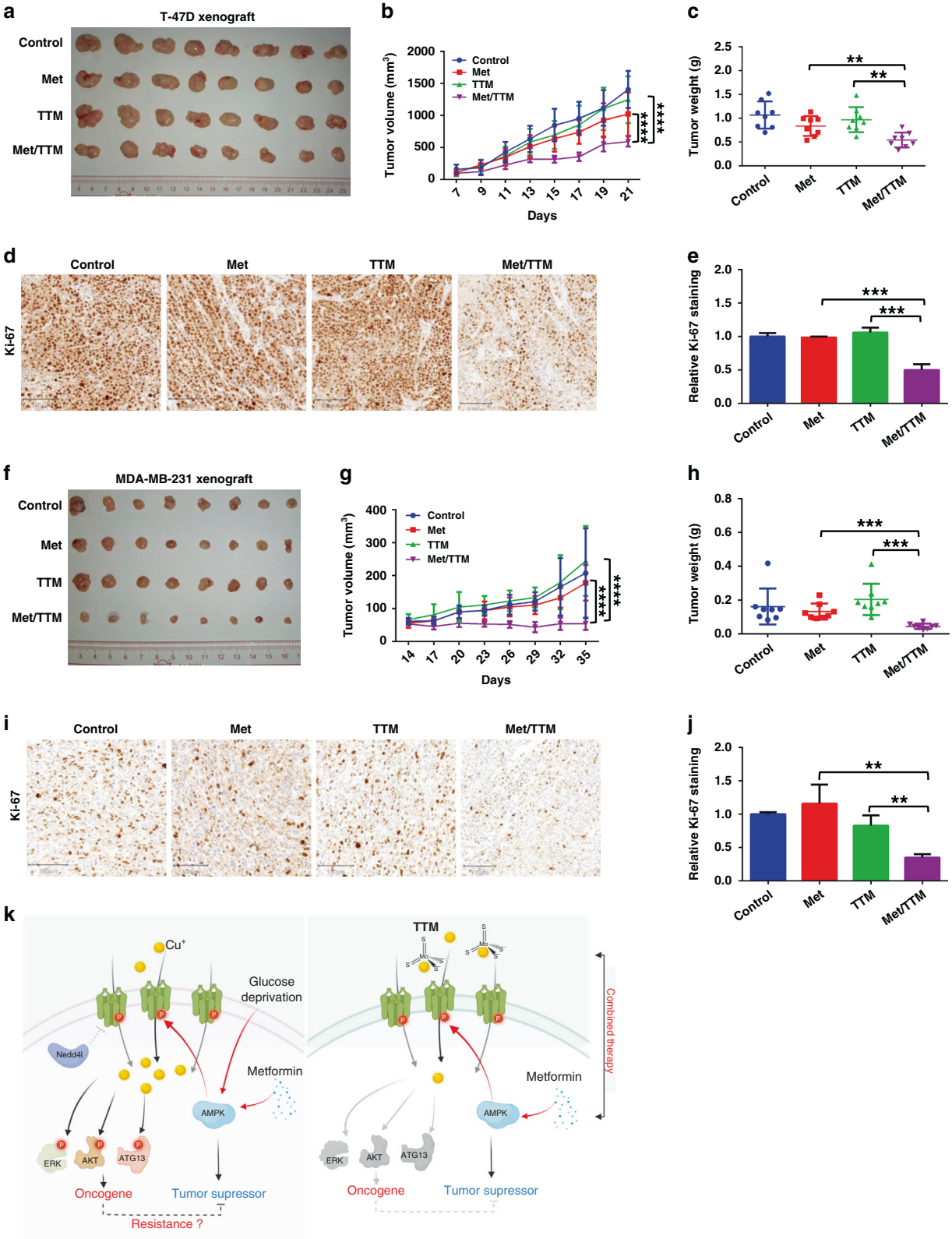

SYBR® Green Premix Pro Taq HS qPCR Kit II (Rox Plus) (AG11719). The primers are listed below:

Forward primer- hCTR1: CAACCTTCTCACCATCACCC
Reverse primer- hCTR1: AGTTCCACATTCTTAAAGCCAAAG
Forward primer- hActin: CATGTACGTTGCTATCCAGGC
Reverse primer- hActin: CTCCTTAATGTCACGCACGAT

Mass spectrometry

Gel bands of proteins with catalase activity were excised for in gel digestion, and proteins were identified by mass spectrometry as previously described [53]. Briefly, proteins were disulfide reduced with 5 mM dithiothreitol (DTT) and alkylated with 11 mM iodoacetamide. In-gel digestion was performed using sequencing

Fig. 7 Metformin synergises with copper chelator TTM in vivo. a–e T-47D cells were subject to xenograft assays. The tumour size was monitored (mean ± SD, $n = 8$) (*$P < 0.05$, ANOVA test) (**a** and **b**). The tumours were dissected and weighed (mean ± SD, $n = 8$). *$P < 0.05$, **$P < 0.01$ (Student's *t*-test) (**c**). The tumour sections were subject to IHC assay with anti-Ki-67 antibody and the images were analysed and calculated (**d** and **e**) (mean ± SD, $n = 3$). *$P < 0.05$, **$P < 0.01$ (Student's *t*-test). Bar indicates 100 μm. **f–j** MDA-MB-231 cells were subjected to xenograft assays. The tumour size was monitored (mean ± SD, $n = 8$) (*$P < 0.05$, ANOVA test) (**f** and **g**). The tumours were dissected and weighed (mean ± SD, $n = 8$). *$P < 0.05$, **$P < 0.01$ (Student's *t*-test) (**h**). The tumour sections were subject to IHC assay with anti-Ki-67 antibody and the images were analysed and calculated (**i** and **j**) (mean ± SD, $n = 3$). *$P < 0.05$, **$P < 0.01$ (Student's *t*-test). Bar indicates 100 μm. **k** A proposed model for the potential roles of AMPK-CTR1-copper axis in breast cancer. Physiological activation of AMPK by glucose deprivation or pathologically by metformin administration could stabilise CTR1, which facilitates copper uptake and activating downstream oncogenic pathways, which possibly antagonises to AMPK tumour suppressor roles (left panel). Thus, this finding provides a strategy to combine AMPK agonist metformin with copper chelator TTM for breast cancer therapies (right panel).

grade-modified trypsin in 50 mM ammonium bicarbonate at 37 °C overnight. The peptides were extracted twice with 1% trifluoroacetic acid in 50% acetonitrile aqueous solution for 1 h. The peptide extracts were then centrifuged in a SpeedVac to reduce the volume. The peptides were resuspended in 20 μl of 0.1% TFA, followed by centrifugation at 20,000 × g at 4 °C for 15 min to remove any particulate impurities.

For LC-MS/MS analysis, peptides were separated by a 40 min gradient elution at a flow rate 0.300 μl/min with a Thermo-Dionex Ultimate 3000 HPLC system, which was directly interfaced with a Thermo Orbitrap Fusion Lumos mass spectrometer. The analytical column was a homemade fused silica capillary column (75 μm ID, 150 mm length; Upchurch, Oak Harbor, WA) packed with C-18 resin (300 A, 5 μm; Varian, Lexington, MA). Mobile phase A consisted of 0.1% formic acid, and mobile phase B consisted of 100% acetonitrile and 0.1% formic acid. An LTQ-Orbitrap mass spectrometer was operated in the data-dependent acquisition mode using Byonic software and there is a single full-scan mass spectrum in the Orbitrap (300–1500 m/z, 120,000 resolution) followed by 3 s data-dependent MS/MS scans in an Ion Routing Multipole at 40% normalised collision energy (HCD).

MS/MS spectra from each LC-MS/MS run were searched against the human database using Proteome Discoverer (Version 1.4) searching algorithm. The search criteria were as follows: full tryptic specificity was required; two missed cleavages were allowed; carbamidomethylation was set as fixed modification; phosphorylation and oxidation (M) were set as variable modifications; precursor ion mass tolerance was 20 ppm for all MS acquired in the Orbitrap mass analyser; and fragment ion mass tolerance was 0.8 Da for all MS2 spectra acquired in the LTQ. High-confidence score filter (FDR < 1%) was used to select the "hit" peptides and their corresponding MS/MS spectra were manually inspected.

Purification of GST-tagged proteins from bacteria

Recombinant GST-CTR1 and GST-CTR1-S105A fragments were generated by transforming the BL21 (DE3) *Escherichia coli* strain. The indicated bacteria were inoculated (the ratio of 1:1000) into 40 ml volumes, respectively. Cultures were grown at 37 °C until an O.D. of 0.8, and then protein expression was induced for 12–16 h using 0.1 mM Isopropyl β-d-1-thiogalactopyranoside at 16 °C with vigorous shaking. Bacteria pellets were collected and resuspended in 5 ml PBS buffer and sonicated to obtain at least 50% output. Following centrifugation, each 1 ml supernatant was incubated with 50 μl of 50% Glutathione-Sepharose slurry for 4 h at 4 °C. The Glutathione beads were washed four times with PBS buffer and eluted by elution buffer (50 mM Tris-HCl, 10 mM reduced glutathione, pH 8.0) at RT. Yield of the desired proteins was confirmed by analysing 10 μl beads by coomassie blue staining and quantified against BSA standards.

In vitro kinase assay

CTR1 in vitro kinase assays were performed from a protocol according to the manufacturer's instructions by an AKT Kinase Assay Kit purchased from Cell Signaling Technology. Briefly, 1 μg of the bacterially purified GST-CTR1 and GST-CTR-S105A fusion proteins were incubated with 50 ng AMPK kinase (Promega, V4012) or immunoprecipitated AMPKα1β1γ2 from glucose-deprived HEK293T in the kinase buffer (200 μM ATP, 100 ng/μl ATP-γ-S, 50 mM Tris pH 7.5, 1 μM $MnCl_2$, 2 mM DTT, 1 mM EGTA) for 30 min at 30 °C. The reaction was subsequently stopped by the addition of 5 × SDS loading buffer or added with 30 mM EDTA and 50 mM p-Nitrobenzyl mesylate at RT for 2 h, and then resolved by SDS-PAGE for immunoblot analysis with indicated antibodies. Furthermore, immunoprecipitated GST-CTR1 and GST-CTR1-S105A were also incubated with immunoprecipitated AMPKα1β1γ2 glucose-deprived HEK293T in the kinase buffer with a similar protocol as done above.

In vivo ubiquitination assay

His-ubiquitin, Nedd4l-ΔC2, and CTR1 were transfected into HEK293T cells. After transfection for 36 h, cells were treated with a combination AMPK agonists or inhibitor with 10 μM carbobenzoxy-Leu-Leu-leucinal (MG132) for 7 h. The cells were disposed, and the ubiquitination was detected according to the procedures of in vivo ubiquitination assay as reported previously [12].

Colony formation assays

Cells were seeded into 6-well plates (300 or 600 cells per well) and treated with the indicated concentration of metformin and TTM, following left for 8–14 days until the formation of visible colonies. Colonies were washed with PBS and fixed with 10% acetic acid/10% methanol for 2 h at RT, and then stained with 0.4% crystal violet in 20% ethanol for 2 h. Next, the plates were washed and air-dried, and colony numbers were counted with ImageJ software.

Cell apoptosis

Cells were treated with the indicated concentration of metformin or AICAR and TTM individually or in combination for the indicated time points. And then, the resulting cells were collected and stained using Annexin V-FITC/PI Apoptosis Detection Kit (Vazyme, A211-01) according to the manufacturer's instructions. Stained cells were analysed by flow cytometry.

EdU staining

Distinct breast cancer cells were inoculated in the 96-well plate and treated with the indicated concentration of metformin or AICAR and TTM individually and in combination for the indicated time points. Following incubation with 50 μM EdU solution for 2 h, cells were disposed using Cell-Light EdU Apollo488 In Vitro Kit (RIBOBO, C10310-3) and analysed by fluorescence microscope (OLYMPUS). Quantification of the fluorescent intensity was performed with ImageJ software.

Xenograft mouse study

Mouse xenograft assays were performed as previously described [12]. Briefly, 2×10^6 T-47D cells or 4×10^6 MDA-MB-231 cells were respectively injected into the flank of female nude mice (8/group, GuangDong GemPharmatech Co., Ltd, 4 weeks of age). Once the tumour size reached 50–100 mm^3, mice were divided into four groups. Besides control group, other groups were individually or in

combination administered with metformin by intraperitoneal injection or TTM by gavage. Metformin at a dose of 150 mg/kg and/or TTM at a dose of 2 mg was administered every day for T-47D xenografted mice, whereas metformin at a dose of 100 mg/kg and/or TTM at a dose of 1.5 mg/kg was administered every day for MDA-MB-231 xenografted mice. Tumour size of T-47D and MDA-MB-231 xenografted mice was measured every 2 or 3 days with a caliper. The tumour volume was determined with the formula: $L \times W^2 \times 0.52$, where L is the longest diameter and W is the shortest diameter. All animal experimental procedures were approved by the Institutional Animal Care and Use Committee of Sun Yat-sen University.

Quantification and statistical analyses

GraphPad Prism version 6.0 was used for statistical analyses. For all experiments, data were analysed by two-tailed Student's *t*-test, one-way analysis of variance (ANOVA) test and two-way ANOVA test. *N* represents repeats of the experiment. Values of $P < 0.05$ were considered statistically significant.

DATA AVAILABILITY

Data are available on request to the authors.

REFERENCES

1. Waks AG, Winer EP. Breast cancer treatment: a review. JAMA. 2019;321:288–300.
2. Denkert C, Liedtke C, Tutt A, von Minckwitz G. Molecular alterations in triple-negative breast cancer-the road to new treatment strategies. Lancet. 2017;389:2430–42.
3. Foulkes WD, Smith IE, Reis-Filho JS. Triple-negative breast cancer. N Engl J Med. 2010;363:1938–48.
4. Masuda H, Baggerly KA, Wang Y, Zhang Y, Gonzalez-Angulo AM, Meric-Bernstam F, et al. Differential response to neoadjuvant chemotherapy among 7 triple-negative breast cancer molecular subtypes. Clin Cancer Res. 2013;19:5533–40.
5. Winters S, Martin C, Murphy D, Shokar NK. Breast cancer epidemiology, prevention, and screening. Prog Mol Biol Transl Sci. 2017;151:1–32.
6. Harbeck N, Penault-Llorca F, Cortes J, Gnant M, Houssami N, Poortmans P, et al. Breast cancer. Nat Rev Dis Prim. 2019;5:66.
7. Schmid P, Adams S, Rugo HS, Schneeweiss A, Barrios CH, Iwata H, et al. Atezolizumab and Nab-Paclitaxel in advanced triple-negative breast cancer. N Engl J Med. 2018;379:2108–21.
8. Feng Y, Zeng JW, Ma Q, Zhang S, Tang J, Feng JF. Serum copper and zinc levels in breast cancer: a meta-analysis. J Trace Elem Med Biol. 2020;62:126629.
9. Lopez J, Ramchandani D, Vahdat L. Copper depletion as a therapeutic strategy in cancer. Met Ions Life Sci. 2019;19.
10. Myint ZW, Oo TH, Thein KZ, Tun AM, Saeed H. Copper deficiency anemia: review article. Ann Hematol. 2018;97:1527–34.
11. Brady DC, Crowe MS, Turski ML, Hobbs GA, Yao X, Chaikuad A, et al. Copper is required for oncogenic BRAF signalling and tumorigenesis. Nature. 2014;509:492–6.
12. Guo J, Cheng J, Zheng N, Zhang X, Dai X, Zhang L, et al. Copper promotes tumorigenesis by activating the PDK1-AKT oncogenic pathway in a copper transporter 1 dependent manner. Adv Sci (Weinh). 2021;8:e2004303.
13. Tsang T, Posimo JM, Gudiel AA, Cicchini M, Feldser DM, Brady DC. Copper is an essential regulator of the autophagic kinases ULK1/2 to drive lung adenocarcinoma. Nat Cell Biol. 2020;22:412–24.
14. Voli F, Valli E, Lerra L, Kimpton K, Saletta F, Giorgi FM, et al. Intratumoral copper modulates PD-L1 expression and influences tumor immune evasion. Cancer Res. 2020;80:4129–44.
15. Rieber M. Cancer pro-oxidant therapy through copper redox cycling: repurposing disulfiram and tetrathiomolybdate. Curr Pharm Des. 2020;26:4461–6.
16. Quinn BJ, Kitagawa H, Memmott RM, Gills JJ, Dennis PA. Repositioning metformin for cancer prevention and treatment. Trends Endocrinol Metab. 2013;24:469–80.
17. Rattan R, Giri S, Singh AK, Singh I. 5-Aminoimidazole-4-carboxamide-1-beta-D-ribofuranoside inhibits cancer cell proliferation in vitro and in vivo via AMP-activated protein kinase. J Biol Chem. 2005;280:39582–93.
18. Lee YK, Park OJ. Regulation of mutual inhibitory activities between AMPK and Akt with quercetin in MCF-7 breast cancer cells. Oncol Rep. 2010;24:1493–7.
19. Ponnusamy L, Natarajan SR, Thangaraj K, Manoharan R. Therapeutic aspects of AMPK in breast cancer: progress, challenges, and future directions. Biochim Biophys Acta Rev Cancer. 2020;1874:188379.
20. Jiralerspong S, Palla SL, Giordano SH, Meric-Bernstam F, Liedtke C, Barnett CM, et al. Metformin and pathologic complete responses to neoadjuvant chemotherapy in diabetic patients with breast cancer. J Clin Oncol. 2009;27:3297–302.
21. Liu B, Fan Z, Edgerton SM, Deng XS, Alimova IN, Lind SE, et al. Metformin induces unique biological and molecular responses in triple negative breast cancer cells. Cell Cycle. 2009;8:2031–40.
22. Lega IC, Fung K, Austin PC, Lipscombe LL. Metformin and breast cancer stage at diagnosis: a population-based study. Curr Oncol. 2017;24:e85–e91.
23. Scherbakov AM, Sorokin DV, Tatarskiy VV Jr, Prokhorov NS, Semina SE, Berstein LM, et al. The phenomenon of acquired resistance to metformin in breast cancer cells: the interaction of growth pathways and estrogen receptor signaling. IUBMB Life. 2016;68:281–92.
24. Jiang Q, Zheng N, Bu L, Zhang X, Zhang X, Wu Y, et al. SPOP-mediated ubiquitination and degradation of PDK1 suppresses AKT kinase activity and oncogenic functions. Mol Cancer. 2021;20:100.
25. Bertinato J, L'Abbe MR. Copper modulates the degradation of copper chaperone for Cu,Zn superoxide dismutase by the 26 S proteosome. J Biol Chem. 2003;278:35071–8.
26. West EC, Prohaska JR. Cu,Zn-superoxide dismutase is lower and copper chaperone CCS is higher in erythrocytes of copper-deficient rats and mice. Exp Biol Med (Maywood). 2004;229:756–64.
27. Caruano-Yzermans AL, Bartnikas TB, Gitlin JD. Mechanisms of the copper-dependent turnover of the copper chaperone for superoxide dismutase. J Biol Chem. 2006;281:13581–7.
28. Herzig S, Shaw RJ. AMPK: guardian of metabolism and mitochondrial homeostasis. Nat Rev Mol Cell Biol. 2018;19:121–35.
29. Clifford RJ, Maryon EB, Kaplan JH. Dynamic internalization and recycling of a metal ion transporter: Cu homeostasis and CTR1, the human Cu(+) uptake system. J Cell Sci. 2016;129:1711–21.
30. Puig S, Thiele DJ. Molecular mechanisms of copper uptake and distribution. Curr Opin Chem Biol. 2002;6:171–80.
31. Maryon EB, Molloy SA, Zimnicka AM, Kaplan JH. Copper entry into human cells: progress and unanswered questions. Biometals. 2007;20:355–64.
32. Mandal T, Kar S, Maji S, Sen S, Gupta A. Structural and functional diversity among the members of CTR, the membrane copper transporter family. J Membr Biol. 2020;253:459–68.
33. Nose Y, Wood LK, Kim BE, Prohaska JR, Fry RS, Spears JW, et al. Ctr1 is an apical copper transporter in mammalian intestinal epithelial cells in vivo that is controlled at the level of protein stability. J Biol Chem. 2010;285:32385–92.
34. Petris MJ, Smith K, Lee J, Thiele DJ. Copper-stimulated endocytosis and degradation of the human copper transporter, hCtr1. J Biol Chem. 2003;278:9639–46.
35. Trefts E, Shaw RJ. AMPK: restoring metabolic homeostasis over space and time. Mol Cell. 2021;81:3677–90.
36. Cheng J, Zhang T, Ji H, Tao K, Guo J, Wei W. Functional characterization of AMP-activated protein kinase signaling in tumorigenesis. Biochim Biophys Acta. 2016;1866:232–51.
37. Amano T, Nakamizo A, Mishra SK, Gumin J, Shinojima N, Sawaya R, et al. Simultaneous phosphorylation of p53 at serine 15 and 20 induces apoptosis in human glioma cells by increasing expression of pro-apoptotic genes. J Neurooncol. 2009;92:357–71.
38. Faria J, Negalha G, Azevedo A, Martel F. Metformin and breast cancer: molecular targets. J Mammary Gland Biol Neoplasia. 2019;24:111–23.
39. De A, Kuppusamy G. Metformin in breast cancer: preclinical and clinical evidence. Curr Probl Cancer. 2020;44:100488.
40. Sammons S, Brady D, Vahdat L, Salama AK. Copper suppression as cancer therapy: the rationale for copper chelating agents in BRAF(V600) mutated melanoma. Melanoma Manag. 2016;3:207–16.
41. Xu M, Casio M, Range DE, Sosa JA, Counter CM. Copper chelation as targeted therapy in a mouse model of oncogenic BRAF-driven papillary thyroid cancer. Clin Cancer Res. 2018;24:4271–81.
42. Ramchandani D, Berisa M, Tavarez DA, Li Z, Miele M, Bai Y, et al. Copper depletion modulates mitochondrial oxidative phosphorylation to impair triple negative breast cancer metastasis. Nat Commun. 2021;12:7311.
43. Shaw RJ, Lamia KA, Vasquez D, Koo SH, Bardeesy N, Depinho RA, et al. The kinase LKB1 mediates glucose homeostasis in liver and therapeutic effects of metformin. Science. 2005;310:1642–6.
44. Snima KS, Pillai P, Cherian AM, Nair SV, Lakshmanan VK. Anti-diabetic drug metformin: challenges and perspectives for cancer therapy. Curr Cancer Drug Targets. 2014;14:727–36.
45. Shaw RJ, Bardeesy N, Manning BD, Lopez L, Kosmatka M, DePinho RA, et al. The LKB1 tumor suppressor negatively regulates mTOR signaling. Cancer Cell. 2004;6:91–9.
46. Shaw RJ, Kosmatka M, Bardeesy N, Hurley RL, Witters LA, DePinho RA, et al. The tumor suppressor LKB1 kinase directly activates AMP-activated kinase and

regulates apoptosis in response to energy stress. Proc Natl Acad Sci USA. 2004; 101:3329–35.
47. Jeon SM, Chandel NS, Hay N. AMPK regulates NADPH homeostasis to promote tumour cell survival during energy stress. Nature. 2012;485:661–5.
48. Laderoute KR, Amin K, Calaoagan JM, Knapp M, Le T, Orduna J, et al. 5′-AMP-activated protein kinase (AMPK) is induced by low-oxygen and glucose deprivation conditions found in solid-tumor microenvironments. Mol Cell Biol. 2006; 26:5336–47.
49. Saito Y, Chapple RH, Lin A, Kitano A, Nakada D. AMPK protects leukemia-initiating cells in myeloid leukemias from metabolic stress in the bone marrow. Cell Stem Cell. 2015;17:585–96.
50. Pan Q, Bao LW, Kleer CG, Brewer GJ, Merajver SD. Antiangiogenic tetrathiomolybdate enhances the efficacy of doxorubicin against breast carcinoma. Mol Cancer Ther. 2003;2:617–22.
51. Das A, Ash D, Fouda AY, Sudhahar V, Kim YM, Hou Y, et al. Cysteine oxidation of copper transporter CTR1 drives VEGFR2 signalling and angiogenesis. Nat Cell Biol. 2022;24:35–50.
52. Wu Y, Zhou L, Wang X, Lu J, Zhang R, Liang X, et al. A genome-scale CRISPR-Cas9 screening method for protein stability reveals novel regulators of Cdc25A. Cell Discov. 2016;2:16014.
53. Domon B, Aebersold R. Mass spectrometry and protein analysis. Science. 2006; 312:212–7.

ACKNOWLEDGEMENTS

We thank members of the Guo laboratory for critical reading and kind suggestions for the manuscript. We thank Xiaolin Tian and Dr Haiteng Deng in Center of Protein Analysis Technology, Tsinghua University, for MS analysis. This work was supported by National Natural Science Foundation of China to JG (32070767, 31871410), China Postdoctoral Science Foundation (XZ, 2020M672954).

AUTHOR CONTRIBUTIONS

This study was conceived and designed by JG and XZ. Development of methodology: XZ and QJ. Acquisition of data (provided animals, acquired and managed patients, provided facilities, etc.): XZ, QJ, YS, LB. Analysis and interpretation of data (e.g., statistical analysis, biostatistics, computational analysis): XZ, QJ, YS, LB. Writing, review, and/or revision of the manuscript: JG, XZ, QJ, YL. Administrative, technical, or material support (i.e., reporting or organising data, constructing databases): WX, XW, BG, ZS, LW. Study supervision: JG, WX, YL. Approved manuscript: all authors.

COMPETING INTERESTS

The authors declare no competing interests.

ETHICS APPROVAL AND CONSENT TO PARTICIPATE

All procedures followed are in accordance with the ethical standards approved by the Institutional Animal Care and Use Committee of Sun Yat-sen University.

ADDITIONAL INFORMATION

Supplementary information The online version contains supplementary material available at https://doi.org/10.1038/s41416-022-02127-4.

Correspondence and requests for materials should be addressed to Ying Lin, Wei Xie or Jianping Guo.